Supplemental Material

Assessment of arrhythmia mechanism and burden of the infarcted ventricles following remuscularization with pluripotent stem cell-derived cardiomyocyte patches using patient-derived models

Joseph K. Yu[1,2,6,7*], Jialiu A. Liang[1,2], William H. Franceschi[1,2], Qinwen Huang[1,2], Farhad Pashakhanloo[2], Eric Sung[2,6,7], Patrick M. Boyle[2,3,4,5], Natalia A. Trayanova[2,6,7]

Affiliations:

[1] Institute for Computational Medicine, Johns Hopkins University, 3400 N Charles Street, 208 Hackerman, Baltimore, MD 21218, USA

[2] Department of Biomedical Engineering, Johns Hopkins University, 3400 N Charles Street, 208 Hackerman, Baltimore, MD 21218, USA

[3] Department of Bioengineering, University of Washington, Seattle, WA, USA

[4] Institute for Stem Cell and Regenerative Medicine, University of Washington, Seattle, WA, USA

[5] Center for Cardiovascular Biology, University of Washington, Seattle, WA, USA

[6] Department of Medicine, Johns Hopkins University School of Medicine, Baltimore, MD, USA

[7] Alliance for Cardiovascular Diagnostic and Treatment Innovation (ADVANCE), Johns Hopkins University, 3400 N Charles Street, 216 Hackerman, Baltimore, MD, USA

[*] Corresponding author. Tel: +1 410 516 4375; Fax: +1 410 516 5294; E-mail: jyu78@jhu.edu

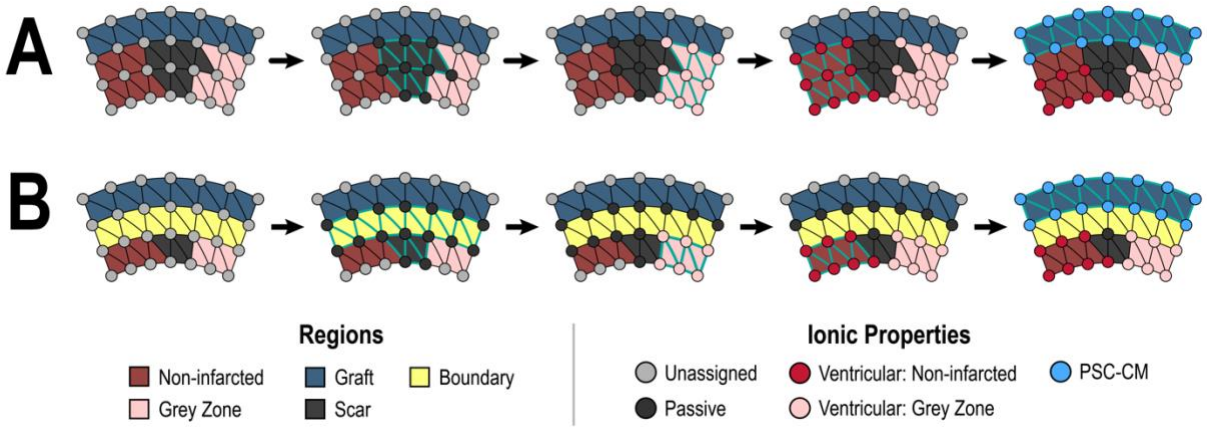

Figure S1: Methodology of simulating complete vs. partial PSC-CM patch engraftment. While host-patch interactions are dictated by the underlying myocardial substrate in **(A)** complete engraftment, host-patch interactions are dictated by a separate designated tissue conductivity in **(B)** partial engraftment. Ionic properties are sequentially assigned (left to right) to specific nodes (circles) based on the corresponding element region types; assignments are highlighted for elements outlined in turquoise. Previous node assignments at shared boundaries between regions are overridden by subsequent assignments. Assignment of ionic properties at each specified node remains unchanged between complete and partial patch engraftment, however.

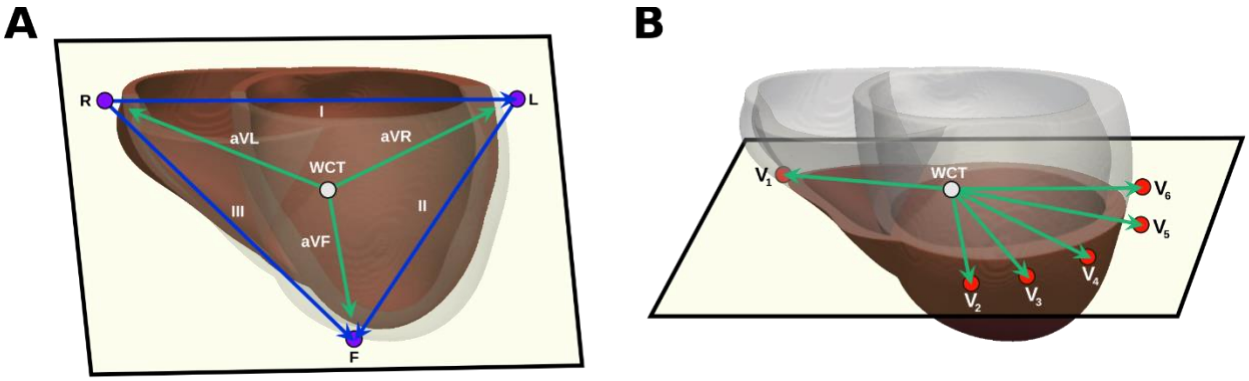

Figure S2. Schematic of pseudo-ECG lead computation.
(A) Einthoven limb lead computation. The left arm (L), right arm (R), and foot (F) unipolar electrode locations (in purple) were approximated with respect to the relative anatomical orientation of the heart and placed 5 mm from the epicardium of the heart. The Wilson Central Terminal (WCT) unipolar electrode location (in white) was computed as the center of mass of L, R, and F (coronal cutting plane shown for clarity). Unipolar signals were computed at the L, R, F, and WCT electrode locations using CARPentry's ECG ϕ_e-recovery method[1]. Bipolar limb leads I, II, and III were then computed by taking the difference between the unipolar signals recorded at L and R, F and L, and F and R, respectively (lead vectors shown in dark blue). Augmented leads aVR, aVL, and aVF were computed by taking linear combinations of leads I, II, and III (lead vectors shown in green) **(B)** Precordial lead computation. Unipolar precordial electrode locations (in red) were approximated with respect to the heart geometry (transverse cutting plane shown for clarity). Unipolar signals were recorded at all precordial electrode locations and the WCT (in white) using CARPentry's ECG ϕ_e-recovery method[1]. Precordial ECG leads were then computed by taking the difference between the unipolar signals at the precordial electrodes and the WCT (lead vectors shown in green).

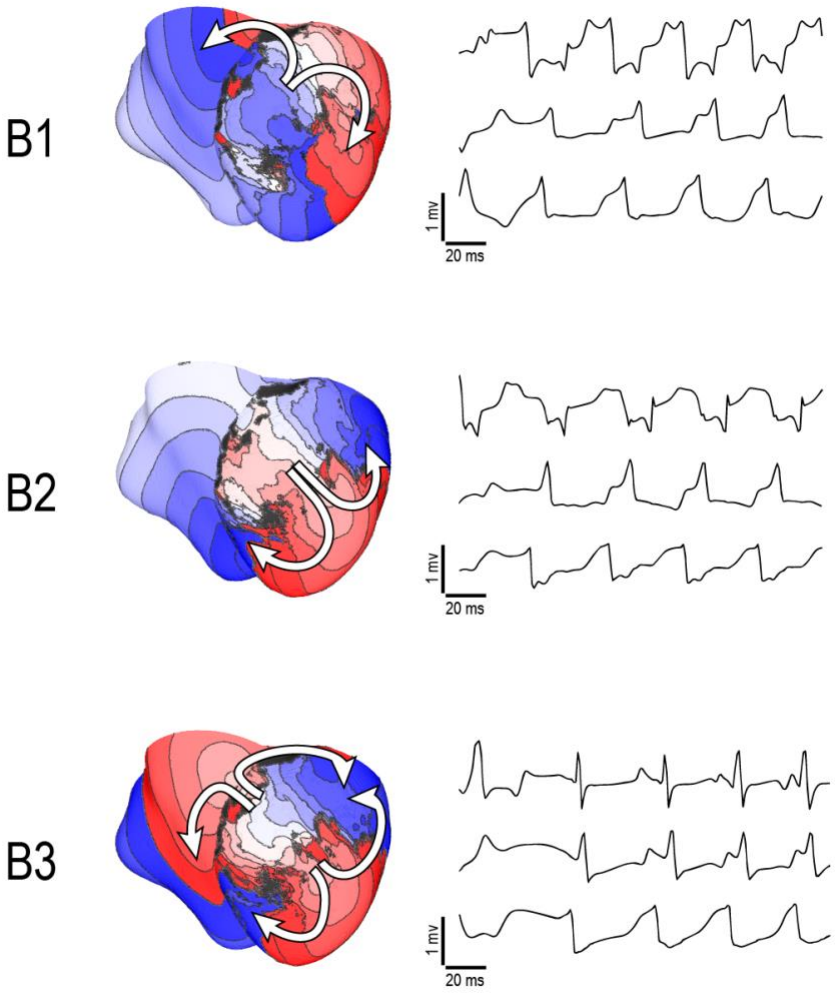

Figure S3: P1 VT morphologies at baseline. Activation maps (left) are shown with pseudo-ECG traces (right) for the three VT morphologies (B1, B2, B3) observed in P1 a baseline.

Figure S4: All VT morphologies observed in P1. Activation maps (left) are shown with pseudo-ECG traces (right) for the all VT morphologies observed in P1. Baseline and emergent morphologies are annotated with a *B* and *E*, respectively.

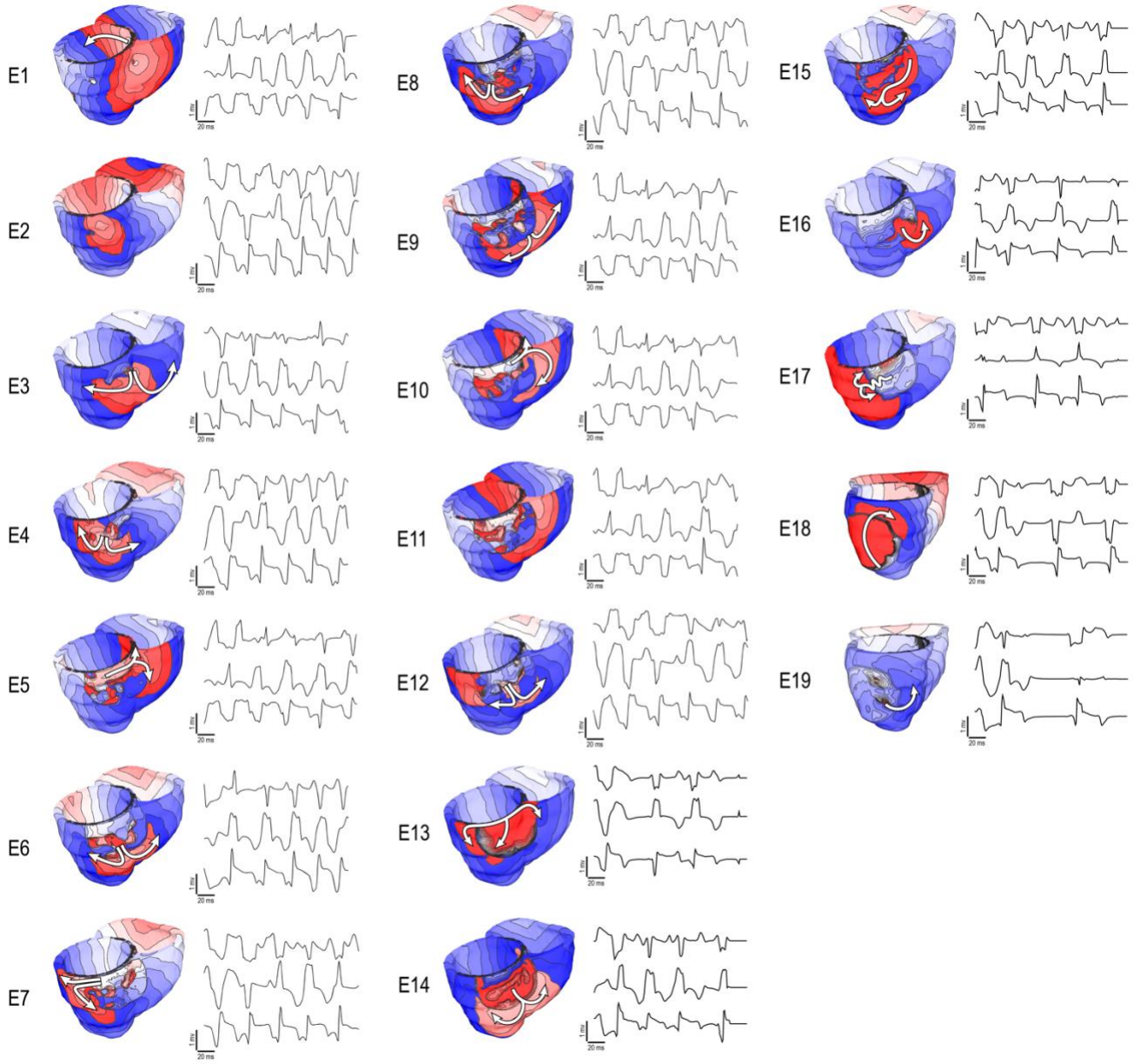

Figure S5: All VT morphologies observed in P2. Activation maps (left) are shown with pseudo-ECG traces (right) for the all VT morphologies observed in P2. P2 was not inducible at baseline so all morphologies were emergent.

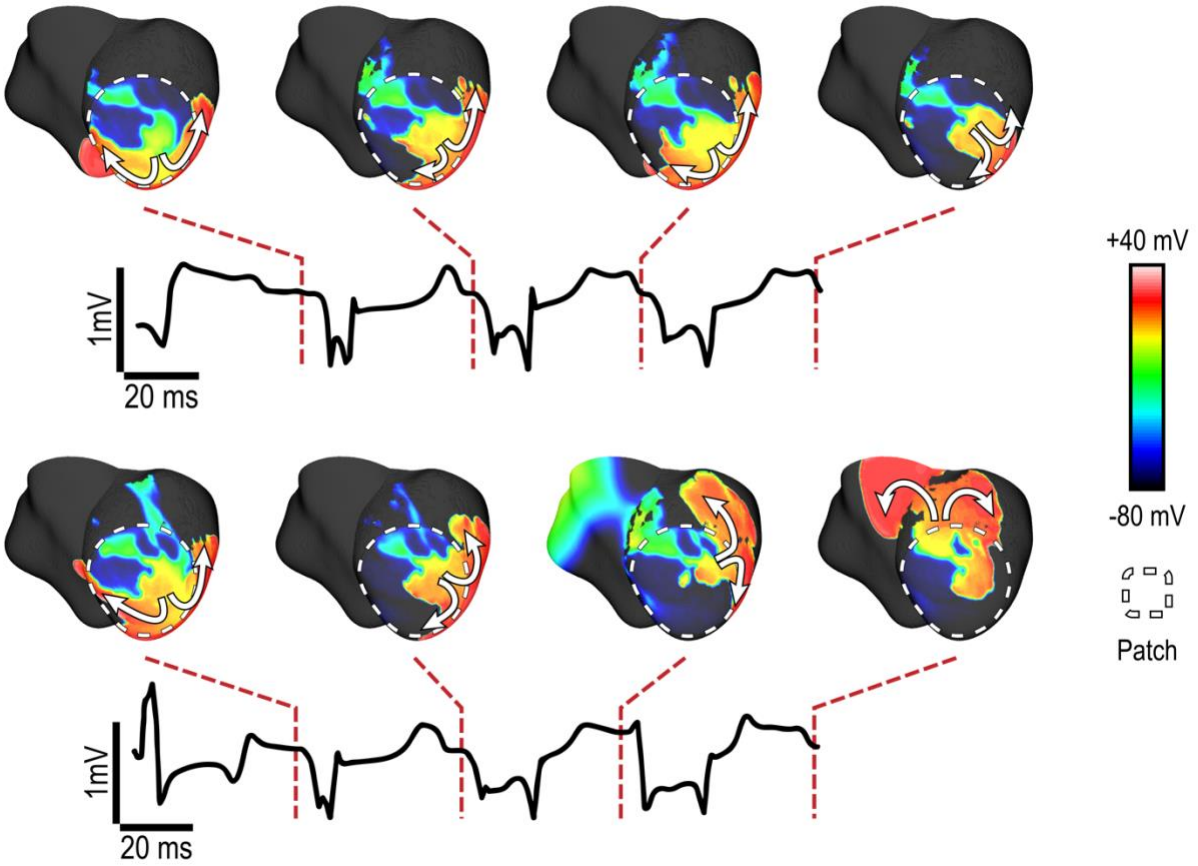

Figure S6: Two distinct VT morphologies observed in P1 when PSC-CM patches were partially engrafted at L1. Transmembrane voltage maps and pseudo-ECGs are shown for each morphology. Voltage maps, taken at regular intervals (indicated by dashed red line), show the reentrant wave at a snapshot in time. One (top) of the VT morphologies resembled baseline VT morphology B2. The other VT morphology (bottom) resembled B2 for the first reentrant cycle only; subsequent reentrant waves meandered around the PSC-CM patch.

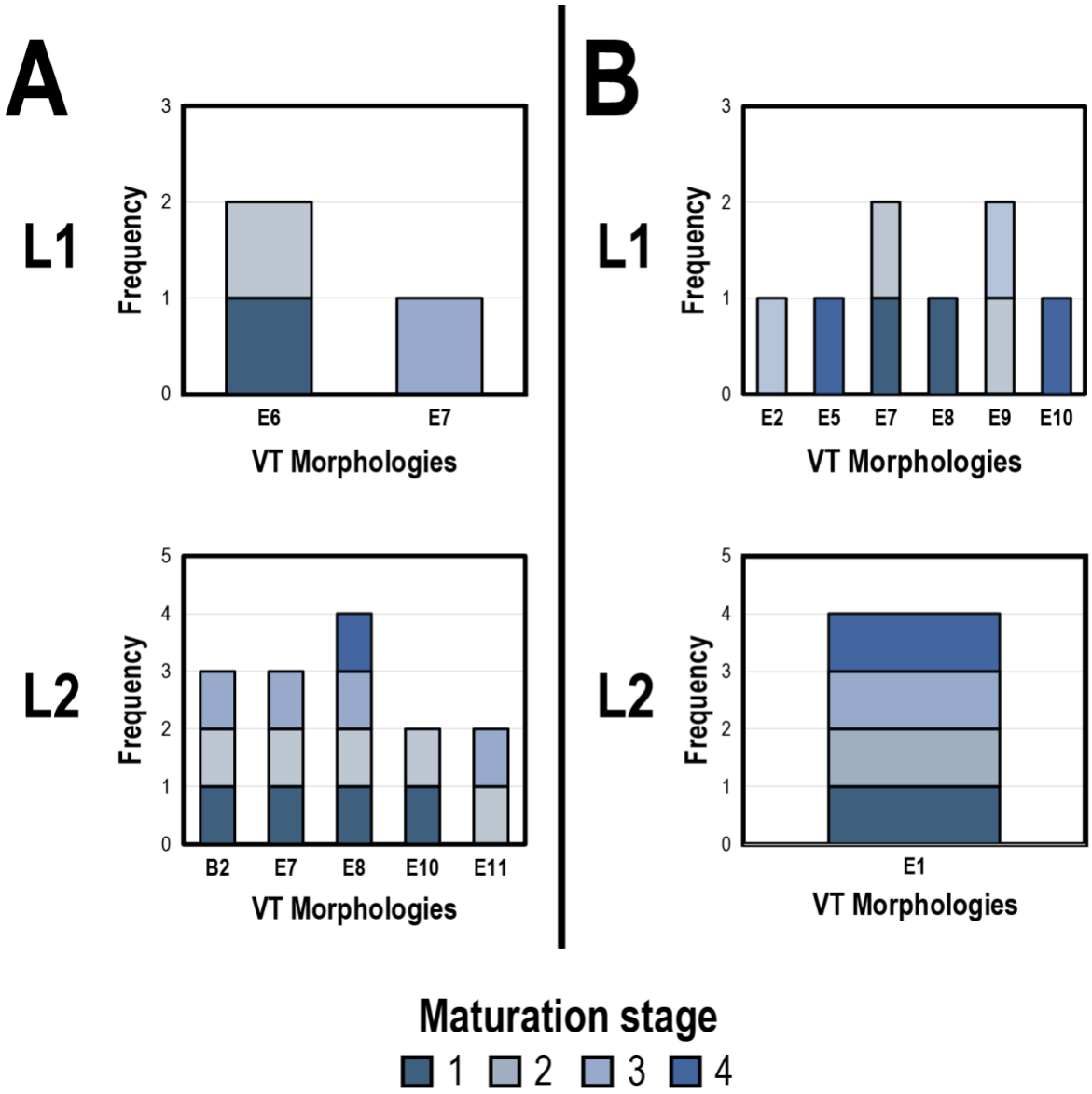

Figure S7: VT dynamics under simulated patch maturation. Frequency of VT morphologies in for remuscularization sites L1 (top) and L2 (top) for **(A)** P1 and **(B)** P2. Colors indicate whether the VT morphology was observed at a given the maturation stage.

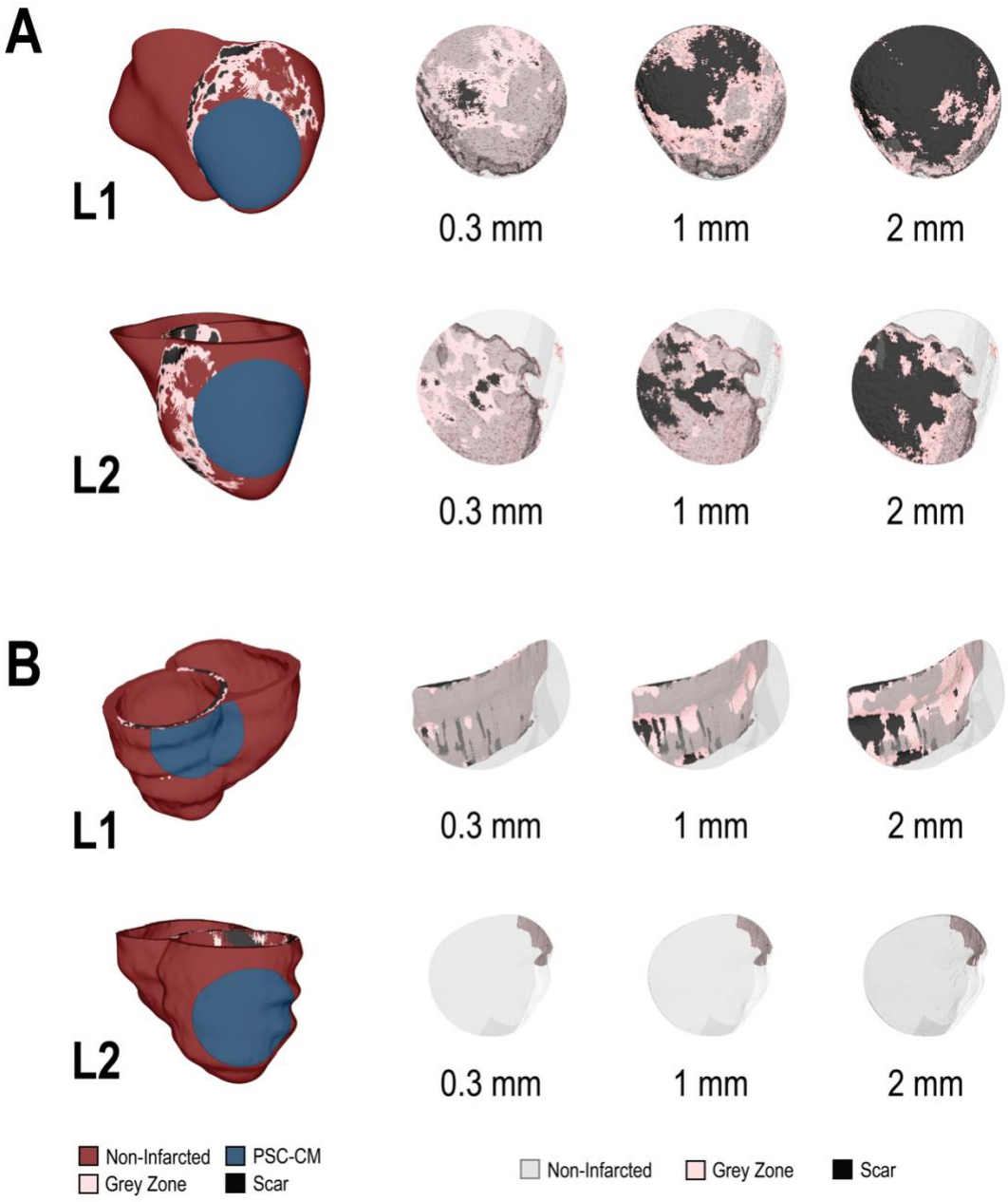

Figure S8: Visualization of patient-specific fibrotic substrate beneath site of remuscularization. Remuscularization at L1 (top) and L2 (bottom) of **(A)** P1 and **(B)** P2. On the left, PSC-CM patches (blue) are visualized with the entire heart models. On the right, the composition of the myocardial wall beneath the patches across various patch depths is shown; non-infarcted myocardium is semi-transparent.

VT morphology	Morphology frequency across different patch dimensions						Total frequency
	Patch depth (radius = 1.6 cm)			**Patch depth,** (radius = 3.2 cm)			
	0.3 mm	**1 mm**	**2 mm**	**0.3 mm**	**1 mm**	**2 mm**	
B1	--	1	--	--	--	--	1
B2	1	1	--	1	--	--	3
E1	1	--	--	--	--	--	1
E3	--	--	1	--	--	--	1
E4	1	--	--	--	--	--	1
E6	--	--	--	1	1	--	2
E7	--	--	--	1	--	1	2
E8	--	--	--	1	--	--	1
E10	--	--	--	1	--	--	1
E12	--	3	8	--	13	8	32
E13	--	1	1	--	--	--	2
E14	--	2	--	--	--	--	2
E15	--	1	--	--	2	--	3
E16	--	--	1	--	--	--	1
E17	--	--	--	--	--	7	7
E18	--	--	--	--	2	--	2
E19	--	--	--	--	1	--	1

Table S1: Frequency of VT morphologies in P1 across different patch dimensions.

VT morphology	Morphology frequency across different patch dimensions						Total Frequency
	Patch depth (radius = 1.6 cm)			**Patch depth** (radius = 3.2 cm)			
	0.3 mm	**1 mm**	**2 mm**	**0.3 mm**	**1 mm**	**2 mm**	
E1	1	2	2	1	1	1	8
E2	1	1	1	--	--	--	3
E3	--	1	1	--	1	--	3
E4	--	1	--	--	--	--	1
E7	--	--	--	1	--	--	1
E8	--	--	--	1	--	--	1
E10	--	--	--	--	--	1	1
E12	--	--	1	--	--	--	1
E13	--	--	--	--	1	6	7
E14	--	--	--	--	1	--	1
E15	--	--	--	--	2	--	2
E16	--	--	--	--	--	3	3
E17	--	--	--	--	--	1	1
E18	--	--	--	--	1	--	1
E19	--	--	--	--	--	1	1

Table S2: Frequency of VT morphologies in P2 across different patch dimensions.

	Maturation stage		Observed VT morphologies and cycle lengths						
			B1	B2	B3	E1	E2	E3	E4
At baseline	--	AVG	376.67	376.67	376.67	--	--	--	--
		STD	50.33	28.87	50.33	--	--	--	--
		Min	330	360	330	--	--	--	--
		Max	430	410	430	--	--	--	--
L1	1	AVG	--	385.33	--	427.78	--	--	429.33
		STD	--	19.59	--	52.08	--	--	79.68
		Min	--	350	--	380	--	--	370
		Max	--	410	--	560	--	--	540
	2	AVG	--	385.33	--	--	410	483.33	430
		STD	--	19.59	--	--	79.37	105.77	80.62
		Min	--	350	--	--	350	370	370
		Max	--	410	--	--	500	650	540
	3	AVG	--	385.33	--	423.33	406.67	--	430
		STD	--	19.59	--	47.91	73.71	--	81.35
		Min	--	350	--	380	350	--	370
		Max	--	410	--	560	490	--	540
L2	1	AVG	--	385.33	--	--	--	--	--
		STD	--	19.59	--	--	--	--	--
		Min	--	350	--	--	--	--	--
		Max	--	410	--	--	--	--	--
	2	AVG	--	371.11	--	--	--	--	423.33
		STD	--	28.92	--	--	--	--	75.72
		Min	--	340	--	--	--	--	370
		Max	--	410	--	--	--	--	510
	3	AVG	--	373.33	--	--	--	--	415
		STD	--	32.02	--	--	--	--	70.07
		Min	--	330	--	--	--	--	330
		Max	--	410	--	--	--	--	500

Table S3: VT cycle lengths in P1 with and without simulated PSC-CM patch (r = 1.6 cm, depth = 0.3 mm)

	Maturation stage		Observed VT morphologies and cycle lengths								
			B1	B2	B3	E6	E7	E8	E9	E10	E11
At baseline	--	AVG	376.67	376.67	376.67	--	--	--	--	--	
		STD	50.33	28.87	50.33	--	--	--	--	--	
		Min	330	360	330	--	--	--	--	--	
		Max	430	410	430	--	--	--	--	--	
L1	1	AVG	--	385.33	--	425.33	--	--	--	--	--
		STD	--	19.59	--	22.64	--	--	--	--	--
		Min	--	350	--	400	--	--	--	--	--
		Max	--	410	--	480	--	--	--	--	--
	2	AVG	--	385.33	--	425	--	--	--	--	--
		STD	--	19.59	--	30.30	--	--	--	--	--
		Min	--	350	--	380	--	--	--	--	--
		Max	--	410	--	460	--	--	--	--	--
	3	AVG	--	385.33	--	436.67	--	--	--	--	--
		STD	--	19.59	--	98.15	--	--	--	--	--
		Min	--	350	--	380	--	--	--	--	--
		Max	--	410	--	550	--	--	--	--	--
L2	1	AVG	--	414.67	--	--	432.00	415.00	473.33	408.33	410
		STD	--	90.23	--	--	51.99	90.06	123.42	37.38	52.92
		Min	--	330	--	--	360	350	370	330	370
		Max	--	550	--	--	500	580	610	470	470
	2	AVG	--	412.67	--	--	439.33	383.33	--	416.67	410
		STD	--	90.27	--	--	51.33	42.50	--	42.71	52.92
		Min	--	320	--	--	360	340	--	330	370
		Max	--	540	--	--	510	440	--	490	470
	3	AVG	--	412.67	--	--	412.67	377.50	441.67	--	410.00
		STD	--	88.36	--	--	59.46	43.09	95.17	--	52.92
		Min	--	330	--	--	320	340	360	--	370
		Max	--	540	--	--	510	440	570	--	470

Table S4: VT cycle lengths in P1 with and without simulated PSC-CM patch (radius = 3.2 cm, depth = 0.3 mm)

Patch radius (cm)	Relative patch conductivity	L1			L2		
		Patch depth (mm)			Patch depth (mm)		
		0.3	1	2	0.3	1	2
1.6	10%	400	500	500	400	500	500
	40%	400	500	500	400	400	400
	100%	400	500	500	400	400	400
3.2	10%	400	500	500	400	500	500
	40%	400	500	500	400	400	500
	100%	400	500	500	300	400	500

Table S5: Minimum pacing interval preserving 1:1 coupling of PSC-CM patch in P1 when subject to decremental electrical pacing. Results are shown for different patch dimensions (radii: 1.6 or 3.2 cm; depth: 0.3, 1, or 2 mm) and patch conductivities (relative) across transplantation sites L1 and L2.

Patch radius (cm)	Relative patch conductivity	L1			L2		
		Patch depth (mm)			Patch depth (mm)		
		0.3	1	2	0.3	1	2
1.6	10%	200	400	500	200	400	500
	40%	200	300	400	200	300	400
	100%	200	300	400	200	300	400
3.2	10%	300	400	500	200	400	500
	40%	200	400	400	200	400	400
	100%	200	400	400	200	400	400

Table S6: Minimum pacing interval preserving 1:1 coupling of PSC-CM patch in P2 when subject to decremental electrical pacing. Results are shown for different patch dimensions (radii: 1.6 or 3.2 cm; depth: 0.3, 1, or 2 mm) and patch conductivities (relative) across transplantation sites L1 and L2.

Supplementary References:

1. Bishop MJ, Plank G. Bidomain ECG simulations using an augmented monodomain model for the cardiac source. *IEEE Trans Biomed Eng* **58**, (2011).